Asian Journal of Convergence in Technology Volume IV Issue I
ISSN NO: 2350-1146 I.F-5.11

A Compact Quad-band Metamaterial Absorber with Wide Incidence Angle for EMI/EMC Applications

Kanwar Preet Kaur and Trushit Upadhyaya
kanwarpreet27@gmail.com

***Abstract*—A compact quad-band metamaterial inspired microwave absorber with wide incidence angle has been reported. The unit cell is composed of L-shaped resonators enclosing a square patch carved on a low cost metal-backed FR-4 dielectric substrate. The optimized absorber exhibits absorption peaks at 1.92GHz, 2.15GHz, 2.44GHz and 2.6GHz thereby covering L-band and S-band frequencies for EMI/EMC applications. The full width at half maxima (FWHM) bandwidth of 19.7% extending from 2.1GHz to 2.56GHz is achieved. The proposed absorber structure shows high absorption under oblique incidence angle up to 45°. The standard printed circuit board (PCB) technique is utilized for fabrication and testing is accomplished by waveguide measurement method. The simulated and measured results are equitable with each other.**

Keywords—metametrials; microwave absorbers; resonators; polarization

I. INTRODUCTION

Metamaterials are artificial material having unconventional properties of negative permittivity, negative permeability and negative refractive index [1-3]. Many metamaterial based applications like resonators [4, 5], antennas [6, 7], filters [8, 9], and energy harvester [10, 11], to name a few, has been reported. Recently, metamaterial inspired absorbers has gained huge interest among researcher because of their attractive properties of frequency scalability [12, 13], ultra-thin [14, 15], compactness [16, 17], enhanced bandwidth [18, 19] as compared to conventional absorbers. Metamaterial absorbers (MMAs) has been utilized for electromagnetic (EM) interference and compatibility issues of radar cross section (RCS) reduction, blocking/absorption of EM signals from mobile phones, local area networks, Wi-Fi networks and terahertz imaging [20-23].

In this article, a compact quad-band metamaterial inspired microwave absorber with wide incidence angle is designed considering EMI/EMC applications for L-band and S-band frequencies. The unit cell of proposed MMA constituting of square patch surrounded by L-shaped resonators is engraved on a metal-backed FR-4 dielectric substrate to obtain light weight and compact absorber. Thickness and size of unit cell at second absorption frequency is $0.024\lambda_0$ and $0.2\lambda_0$, respectively. The absorber is simulated using 3D full wave high frequency structure simulator (HFSS) to achieve absorption peaks of 86.21%, 92.71%, 99.87% and 88.26% at respective four distinct frequencies of 1.92 GHz, 2.15 GHz, 2.44 GHz and 2.6 GHz. Full width at half maxima (FWHM) bandwidth of 19.7% ranging from 2.1 GHz to 2.56 GHz is obtained with peaks of 92.71% and 99.87% at 2.15 GHz and 2.44 GHz, respectively. The standard printed circuit board (PCB) fabrication technique is used to manufacture the proposed absorber prototype. The measurement results are equitable with the numerically simulated results. Furthermore, the proposed structure is studied at various polarization angle and oblique angle. High absorption is achieved for wide oblique incidence angle up to 45°. In addition, the simultaneous existence of the electric and magnetic response in the absorber structure is verified by electric field distributions and surface current distributions at all mentioned absorption frequencies.

II. ABSORBER DESIGN AND NUMERICAL SIMULATION RESULTS

A. Absorber Design

The front view of the proposed absorber structure is shown in Fig. 1 with the applied directions of fields and incident wave. L-shaped resonators enclosing a square patch is imprinted on a 3.2 mm thick FR-4 substrate which is terminated by metal ground plane. The conductivity (σ) and thickness of metal plane are 5.8×10^7 S/m and 0.035mm, respectively. The relative permittivity (ε_r) of the dielectric substrate is 4.4 and loss tangent ($\tan\delta$) is 0.02. The optimized geometrical parameters are as follows (all dimensions are in 'mm'): a=25.6, L_1=25.2, L_2=12.5, g=0.2 and w=1. The absorber structure is simulated by applying periodic boundary conditions via Floquet port excitation in HFSS. Electric and magnetic fields are applied in the direction of x-axis and y-axis with surface normal vectors directed perpendicular to the wave propagation direction.

B. Numerical Absorption Response

Any transmission through the structure is completely blocked by the bottom ground plane which has thickness much greater than its skin depth at guided wavelength. The absorption is calculated from the equation $A(\omega)=1-\left|S_{11}(\omega)\right|^2$ [24]. Hence, reflection coefficient, $R(\omega)=\left|S_{11}(\omega)\right|^2$, is the only factor which is needed to be minimized to achieve high absorption. The impedance of the absorber structure is matched

to the free space impedance at the resonance frequency to reduce R(ω). This matching of impedance is attained by varying geometrical parameters of the design. The peak absorption of 86.21%, 92.71%, 99.87% and 88.26% is obtained at 1.92GHz, 2.15GHz, 2.44GHz and 2.6GHz, respectively, with minor absorption band of 48.27% at 2.87GHz. The simulated absorption response is depicted in Fig. 2. It is observed that FWHM bandwidth of 19.7% is obtained between frequency bands of 2.1GHz to 2.56GHz.

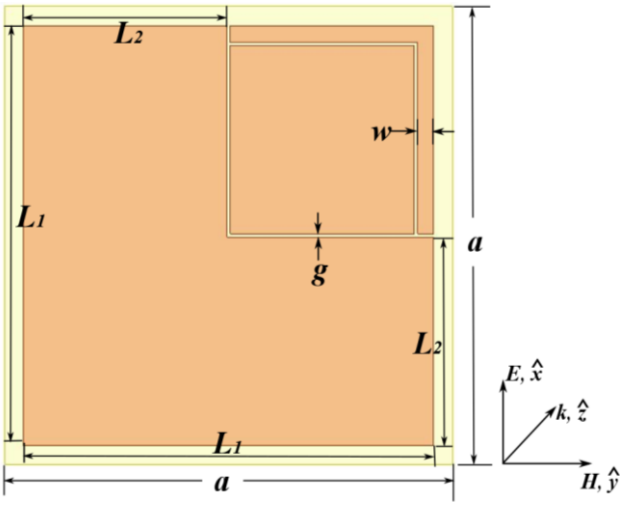

Fig. 1. Top view of the unit cell of the proposed quad-band MMA

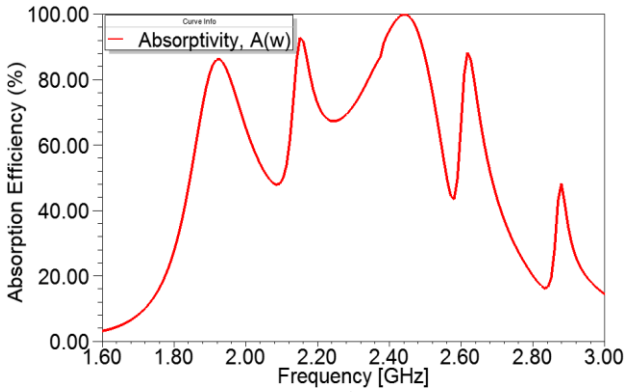

Fig. 2. Simulated absorption response of the proposed quad-band MMA

C. Absorption Mechanism

For better insight in to the absorption mechanism of the presented design the induced electric field distributions and surface current distributions are plotted. Electric field distributions within the structure for all four absorption frequencies are shown in the Fig. 3. It is observed from Fig. 3b that major build-up of the electric field appears at 2.15GHz and 2.44GHz which causes strong absorption of incident EM wave at these frequencies whereas weak electric field is build-up (ref. Fig. 3) at other frequencies results in low absorption of the incident wave. From Fig. 3a, it is evident that weak fields causes least absorption at 1.92GHz. The induced electric field within the absorber structure creates the electric excitation which successively controls effective permittivity. It is also noted that the L-shaped patch is significantly contributing on the absorption response owing to strong accumulation of the electric field around its edges as compared to inverted-L and square patch.

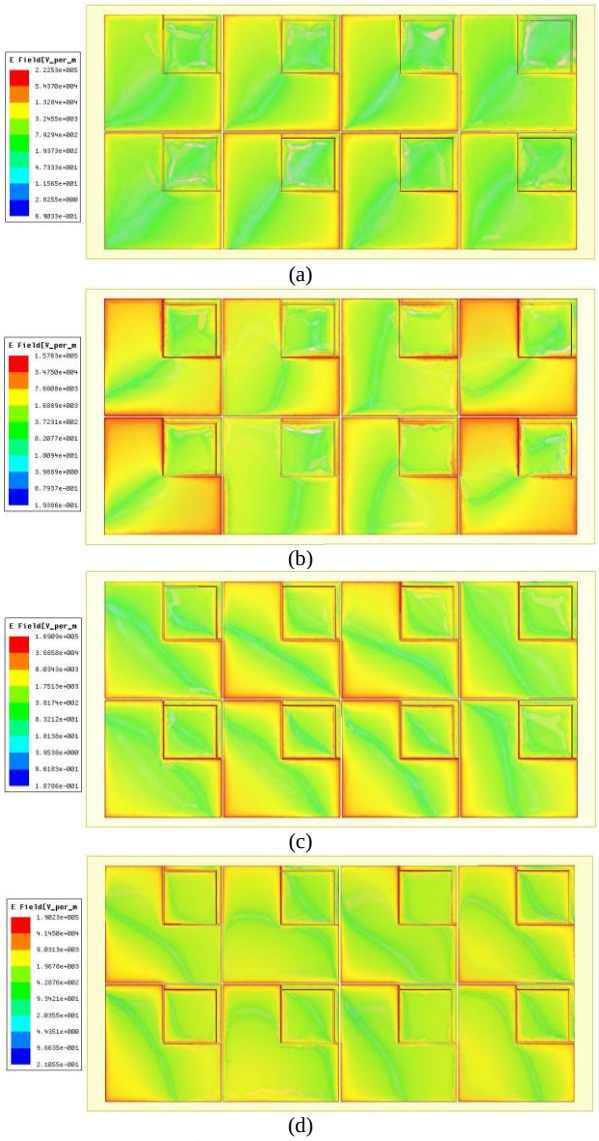

(a)

(b)

(c)

(d)

Fig. 3. Induced Electric field distributions within the proposed quad-band MMA at frequencies of (a) 1.92GHz, (b) 2.15GHz, (b) 2.44GHz, (d)2.6GHz

The surface current distributions at the top and bottom surfaces at four absorption frequencies are presented in Fig. 4 and Fig. 5, respectively. It is observed that the surface currents in the top surface and bottom surface are anti-parallel to each other at all four frequencies. These anti-parallel currents give rise to the circulating current loops which are normal to the incident magnetic field direction. In turn, these circulating current loops create magnetic excitations thereby controlling effective permeability of the structure. The desired absorption response is achieved due to the simultaneous occurrence of the magnetic and electric excitation.

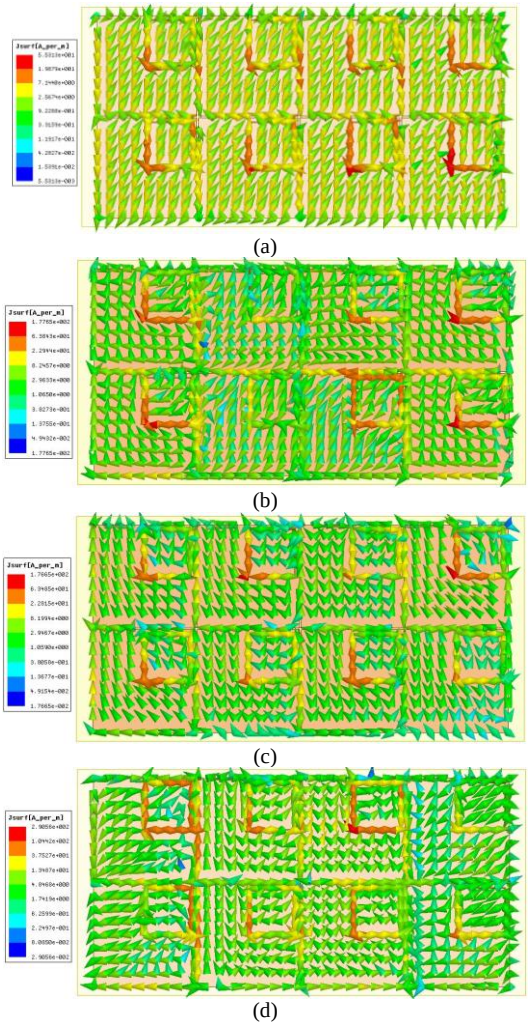

(a) (b) (c) (d)

Fig. 4. Surface current distribution at top surface of the proposed quad-band MMA at frequencies of (a) 1.92GHz, (b) 2.15GHz, (b) 2.44GHz, (d) 2.6GHz

D. Analysis for Polarization and Oblique Incidence Angle

The proposed quad-band MMA structure has been studied for variations in polarization angle (ϕ) under normal incidence. The electric and magnetic fields are varied by ϕ-angle with respect to x-direction and y-direction with wave propagation along z-directions. Due to the single-fold symmetry the absorption response of the proposed design is dependent on the polarization angle. It is observed from Fig. 6a that maximum absorption is obtained only at 0° and 90. Proposed structure has also been investigated for the effects of variations in oblique angles (θ) on absorption response while keeping polarization angle fixed. In this case direction of magnetic/electric field and wave propagation vector are varied by θ-angle simultaneously keeping electric/magnetic vector constant. The simulated absorption responses for various oblique angles are depicted in Fig. 6b. It is evident that the proposed MMA design attains high absorption for variation in θ-angle up to 45°.

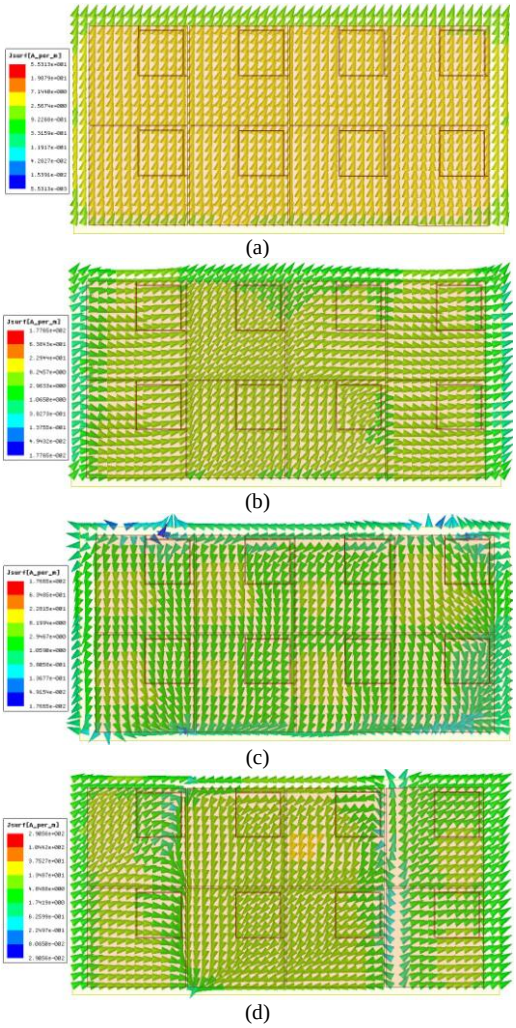

(a) (b) (c) (d)

Fig. 5. Surface current distribution at the bottom surface of the proposed quad-band MMA at frequencies of (a) 1.92GHz, (b) 2.15GHz, (b) 2.44GHz, (d) 2.6GHz

III. Measurement and Results

The proposed absorber structure with 8 unit cells is fabricated on a planar 3mm thick FR4 substrate sheet having dimension of 109.22mm×55.61mm using standard printed circuit board (PCB) technology. The fabricated sample of the proposed design is shown in Fig. 7a. A standard WR-430 waveguide is used to measure the presented absorber which is connected to the Agilent N9912A vector network analyzer (VNA) with RG-142 Teflon coaxial cable.

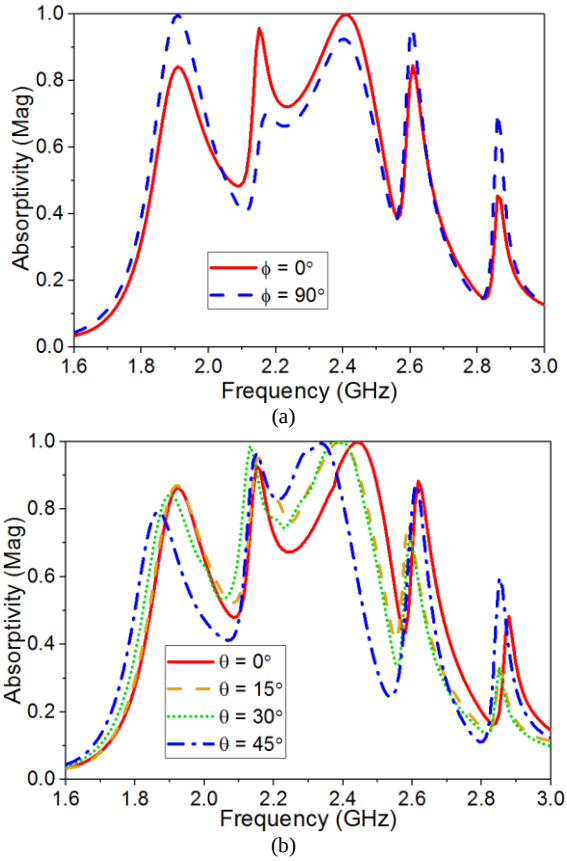

Fig. 6. Simulated absorption response of the quad-band MMA under (a) normal incidence for different polarization angles (b) oblique incidence.

Initially, a copper sheet having dimensions same as that of the fabricated sample is place inside the waveguide and reflection from this sheet is measured. This measured return loss is considered as a reference. Next, the copper sheet is replaced with the fabricated absorber sample and reflection from this fabricated sample is measured. The difference between the reference return loss and the return loss from the fabricated sample gives rise to the actual reflection from the absorber structure. The complete measurement arrangement is shown in Fig. 7b. Fig. 8, illustrates the measured return loss which is compared with the numerically simulated return loss. The measured return loss exists at four distinct frequencies of 1.87 GHz, 2.15 GHz, 2.34 GHz and 2.61 GHz. The measure FWHM absorption bandwidth is obtained as 15.56% ranging from 2.104GHz to 2.459GHz. A significant frequency shift is observed in the measured result which is mainly due to the presence of TE excitation [25, 26] inside the waveguide.

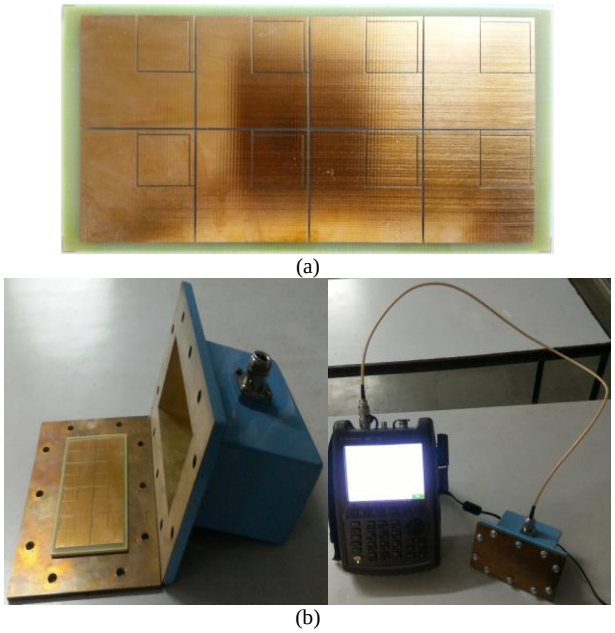

Fig. 7. (a) Fabricated sample of the proposed quad-band MM, (b) Waveguide measurement technique arrangements

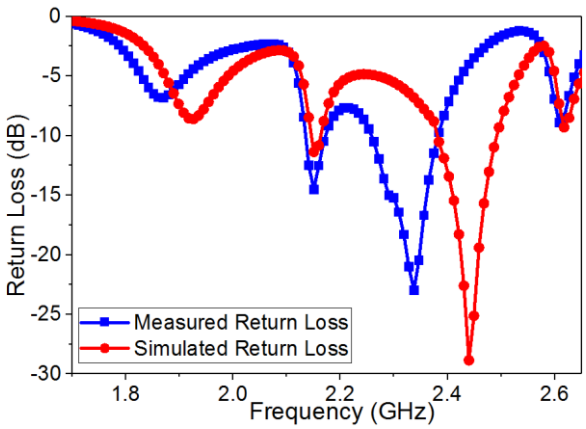

Fig. 8. Measured return loss compared with the simulated return loss of the proposed quad-ban MMA

IV. Conclusion

A compact wide angle quad-band metamaterial absorber composed of L-shaped resonators enclosing a square patch has been proposed in this article. The resonator patches are engraved on low cost FR4 substrate with back metal plane to

exhibit absorption peaks of 86.21%, 92.71%, 99.87% and 88.26% at 1.92 GHz, 2.15 GHz, 2.44 GHz and 2.60 GHz, respectively, thereby covering L-band and S-band frequencies for EMI/EMC applications. The full width at half maxima bandwidth of 19.7% is achieved extending from 2.1 GHz to 2.56 GHz with peaks of 92.71% and 99.87%, respectively. The proposed absorber structure shows high absorption under oblique incidence angle up to 45° while the absorption response depends on the polarization angle due to single-fold symmetry. For better insight in to absorption mechanism of the presented design the induced electric field distributions and surface current distributions are presented. The absorber is tested using waveguide method and the measured results are equitable with the simulated results. The structure is compact with thickness and size less than $0.024\lambda_0$ and $0.2\lambda_0$ with respect to the second absorption frequency.

REFERENCES

[1] V.G. Veselago, "The electrodynamics of substances with simultaneously negative values of ε and μ," *Soviet Physics Uspekhi*, vol. 10, pp. 509–514, 1968.

[2] D.R. Smith, W.J. Padilla, D.C. Vier, S.C. Nemat-Nasser, and S. Schultz, "Composite medium with simultaneously negative permeability and permittivity," *Physical Review Letters*, vol. 84, pp. 4184–4187, 2000.

[3] R.A. Shelby, D.R. Smith, and S. Schultz, "Experimental verification of a negative index of refraction," *Science (New York, N.Y.)*, vol. 292, pp. 77–79, 2001.

[4] T.K. Upadhyaya, S.P. Kosta, R. Jyoti and M. Palandöken, "Negative refractive index material-inspired 90-deg electrically tilted ultra wideband resonator," *Optical Engineering*, vol. 53, pp. 107104–107104, 2014.

[5] M. Palandoken and H. Henke, "Fractal spiral resonator as magnetic metamaterial," in *Applied Electromagnetics Conference (AEMC)-2009*, IEEE, pp. 1–4, 2009.

[6] T.K. Upadhyaya, S.P. Kosta, R. Jyoti,and M. Palandöken, "Novel stacked μ-negative material-loaded antenna for satellite applications," *International Journal of Microwave and Wireless Technologies*, vol. 8, pp. 229–235, 2016.

[7] T.K. Upadhyaya, V.V. Dwivedi, S.P. Kosta, and Y.P. Kosta, "Miniaturization of tri band patch antenna using metamaterials," in *Computational Intelligence and Communication Networks (CICN)-2012 Fourth International Conference*, IEEE, pp. 45–48, 2012.

[8] M. Palandöken and A. Sondas, "Compact Metamaterial Based Bandstop Filter," *Microwave Journal*, vol. 57, pp.76–84, 2014.

[9] M. Palandöken and Mustafa H.B. Ucar, "Compact metamaterial-inspired band-pass filter," *Microwave and Optical Technology Letters*, vol. 56, pp. 2903-2907, 2014.

[10] T.S. Almoneef and O.M. Ramahi, "Metamaterial electromagnetic energy harvester with near unity efficiency," *Applied Physics Letters*, vol. 106, pp. 153902-1–045106-7, 2015.

[11] M. Palandöken, "Microstrip antenna with compact anti-spiral slot resonator for 2.4 GHz energy harvesting applications," *Microwave and Optical Technology Letters*, vol. 58, pp. 1404–1408, 2016.

[12] Y. Cheng, H. Yang, Z. Cheng, and N. Wu, "Perfect metamaterial absorber based on a split-ring-cross resonator," *Applied Physics A: Materials Science and Processing*, vol. 102, pp. 99–103, 2011.

[13] F. Dincer, O. Akgol, M. Karaaslan, E. Unal, and C. Sabah, "Polarization angle independent perfect metamaterial absorbers for solar cell applications in the microwave, infrared, and visible regime," *Progress In Electromagnetics Research*, vol. 144, pp. 93–101, 2014.

[14] S. Bhattacharyya, S. Ghosh, D. Chaurasiya, and V.K. Srivastava, "Bandwidth-enhanced dual-band dual-layer polarization-independent ultra-thin metamaterial absorber," *Applied Physics A: Materials Science and Processing*, vol. 118, pp. 207–215, 2014.

[15] D. Yu, P. Liu, Y. Dong, D. Zhou, and Q. Zhou, "A sextuple-band ultra-thin metamaterial absorber with perfect absorption", *Optics Communications*, vol. 396, pp. 28–35, 2017.

[16] S. Shang, S.Yang,L. Tao, L. Yang, and H.Cao, "Ultrathin triple-band polarization-insensitive wide-angle compact metamaterial absorber," *AIP Advances*, vol. 6, pp. 075203-1–075203-8, 2016.

[17] D. Sood and C. C. Tripathi, "A polarization insensitive compact ultrathin wide-angle penta-band metamaterial absorber," *Journal of Electromagnetic Waves and Applications*, vol. 31, pp. 394–404, 2017.

[18] X. Ling, Z. Xiao, X. Zheng, J. Tang, and K. Xu, "Broadband and polarization-insensitive metamaterial absorber based on hybrid structures in the infrared region," *Journal of Modern Optics*, vol. 64, pp. 665–671, 2017.

[19] S. Ghosh, S. Bhattacharyya, Y. Kaiprath, and V.K. Srivastava, "Bandwidth-enhanced polarization-insensitive microwave metamaterial absorber and its equivalent circuit model," *Journal of Applied Physics*, vol. 115, pp. 104503-1–104503-5, 2014.

[20] H. Oraizi, A. Abdolali, and N. Vaseghi, "Application of double zero metamaterials as radar absorbing materials for the reduction of radar cross section," *Progress In Electromagnetics Research*, vol. 101, pp. 323–337, 2010.

[21] S.A. Kuznetsov, A.G. Paulish, A.V. Gelfand, P.A. Lazorskiy, and V.N. Fedorinin, "Matrix structure of metamaterial absorbers for multispectral terahertz imaging," *Progress In Electromagnetics Research*, vol. 122, pp. 93–103, 2012.

[22] T.M. Kollatou, A.I. Dimitriadis, S. Assimonis, N.V. Kantartzis, and C.S. Antonopoulos, "A family of ultra-thin, polarization-insensitive, multi-band, highly absorbing metamaterial structures," *Progress In Electromagnetics Research*, vol. 136, pp. 579–594, 2013.

[23] A. Shater and D. Zarifi, "Radar cross section reduction of microstrip antenna using dual-band metamaterial absorber," *Applied Computational Electromagnetics Society Journal*, vol. 32, pp. 135–140, 2017.

[24] N.I. Landy, S. Sajuyigbe, J.J. Mock, D.R. Smith, and W.J. Padilla, "Perfect metamaterial absorber," *Physical review letters*, vol. 100, pp. 207402-1–207402-6, 2008.

[25] H. Zhai, C. Zhan, L. Liu, and Y. Zang, "Reconfigurable wideband metamaterial absorber with wide angle and polarisation stability," *Electronics Letters*, vol. 51, pp. 1624–1626, 2015.

[26] K.P. Kaur, T.K. Upadhyaya, and M. Palandoken, "Dual-Band Polarization-Insensitive Metamaterial Inspired Microwave Absorber for LTE-Band Applications," *Progress In Electromagnetics Research C*, vol. 77, pp. 91–100, 2017.